JOURNAL OF SOLID STATE CHEMISTRY 77, 275–280 (1988)

Crystal Chemistry of Cadmium–Zinc Ferrites

C. OTERO AREAN

Departamento de Química, Facultad de Ciencias, Palma de Mallorca 07071, Spain

AND E. GARCIA DIAZ, J. M. RUBIO GONZALEZ, AND M. A. VILLA GARCIA

Departamento de Química Inorgánica, Facultad de Química, Oviedo, Spain

Received February 15, 1988; in revised form July 1, 1988

$CdFe_2O_4$, $ZnFe_2O_4$, and several mixed ferrites $Cd_xZn_{1-x}Fe_2O_4$ were prepared, in polycrystalline form, by solid-state reaction of mixtures of CdO, ZnO, and Fe_2O_3 at 1223 K. The resulting materials were found to have the spinel-type structure. X-ray powder diffractometry was used to determine the unit-cell length, the oxygen parameter, and the distributions of Cd^{2+}, Zn^{2+}, and Fe^{3+} in tetrahedral and octahedral coordination. $CdFe_2O_4$ and $ZnFe_2O_4$ are 14 and 21% inverse, respectively. Up to $x = 0.75$, Cd^{2+} was found to replace Zn^{2+} exclusively at tetrahedral sites. The results are discussed in terms of the tetrahedral preference of the cations involved alongside the lattice distortion caused by steric effects.

Introduction

Ferrites are extensively used as magnetic materials by virtue of their high electrical resistivity and consequently low eddy currents and dielectric loss. They also find wide application in microwave devices, computer memories, and magnetic recording (*1–3*). A key factor in all of these applications is that the properties of ferrites can be controlled in broad measure by the design engineer to suit the purposes of a particular device. The extent to which such control can be exerted depends, however, on a deep understanding of the factors which determine the crystal chemistry and consequent physical properties of these materials.

Many ferrites have the spinel-type structure (*2, 4*) which can be described in terms of a nearly cubic close-packed arrangement of anions with one-half of the octahedral interstices (*B* sites) and one-eighth of the tetrahedral interstices (*A* sites) filled with cations, the space group being $Fd3m$. The general formula of compounds with the spinel structure is AB_2O_4 and there are eight of these units in a unit cell. The ions are located in the following positions:

8 *A* ions at $0,0,0$; $\frac{1}{4},\frac{1}{4},\frac{1}{4}$;

16 *B* ions at $\frac{5}{8},\frac{5}{8},\frac{5}{8}$; $\frac{5}{8},\frac{7}{8},\frac{7}{8}$; $\frac{7}{8},\frac{5}{8},\frac{7}{8}$; $\frac{7}{8},\frac{7}{8},\frac{5}{8}$;

32 anions at u,u,u; $\frac{1}{4}-u, \frac{1}{4}-u, \frac{1}{4}-u$;

$u,\bar{u},\bar{u}$; $\frac{1}{4}-u, \frac{1}{4}+u, \frac{1}{4}+u$;

$\bar{u},u,\bar{u}$; $\frac{1}{4}+u, \frac{1}{4}-u, \frac{1}{4}+u$;

$\bar{u},\bar{u},u$; $\frac{1}{4}+u, \frac{1}{4}+u, \frac{1}{4}-u$,

0022-4596/88 $3.00

with the face-centered translations, equivalent positions (0,0,0; $0,\frac{1}{2},\frac{1}{2}$; $\frac{1}{2},0,\frac{1}{2}$; $\frac{1}{2},\frac{1}{2},0$). In the nonideal structure the anions are displaced from their ideal positions along [111] directions away from the nearest tetrahedral hole. This deviation is quantified by the oxygen parameter, u, which is 0.375 in the ideal structure, but very often takes significantly higher values (*2, 5, 6*).

Cadmium–zinc ferrites, $Cd_xZn_{1-x}Fe_2O_4$, may be regarded as solid solutions between $CdFe_2O_4$ and $ZnFe_2O_4$. Both of these end members are known to have the spinel-type structure with an approximately normal cation distribution (*6*); i.e., the divalent ions (Cd^{2+} and Zn^{2+}) occupy mainly tetrahedral sites. Cation site preferences in binary spinels are well documented (*6–10*), but spinels with three kinds of cations present a more complex situation where cation distribution is generally a function of chemical composition (*11*). The present paper reports a structural investigation of the mixed spinel ferrites $Cd_xZn_{1-x}Fe_2O_4$. X-ray powder diffraction was used to determine the unit-cell length a_0, the oxygen parameter u, and the cation distribution as a function of composition. The system presents the additional interest of having three cations which, individually considered, all show tetrahedral preference in oxide spinels. Thus, Fe^{3+} is known to occupy tetrahedral interstices in most spinel ferrites (*2, 4, 6*); among the exceptions are $CdFe_2O_4$ and $ZnFe_2O_4$ where the tetrahedral preference of the divalent ions outweighs that of Fe^{3+}. Cd^{2+} and Zn^{2+} also occupy tetrahedral sites in gallate (*12*) and aluminate (*13*) spinels.

Experimental

Specimen Preparation

$CdFe_2O_4$, $ZnFe_2O_4$, and four mixed ferrites $Cd_xZn_{1-x}Fe_2O_4$ (x = 0.25, 0.50, 0.75, and 0.85) were prepared in polycrystalline form by solid-state reaction at 1223 ± 20 K of the parent oxides. CdO and ZnO were, respectively, Merck 99.9% and Koch-Light 99.99%; Fe_2O_3 was obtained by thermal decomposition (at 1273 K) of $Fe(NO_3)_3 \cdot 9H_2O$ (Merck 99.5%), the final product being checked by X-ray diffraction. To compensate for loss of CdO, which is appreciably volatile at 1223 K, an excess of this component was added to the initial oxide mixtures; the excess which persists at the end of the reaction was eliminated with dilute acetic acid.

To facilitate reaction the samples were periodically removed from the furnace and reground. This also allowed the progress of the reaction to be followed by X-ray diffraction. When no traces of ZnO or Fe_2O_3 were apparent (typically after 300 hr), the samples were reheated to 1223 K for a further 30 hr to ensure total conversion into the final product. They were then rapidly immersed in liquid nitrogen to quench the cation distribution equilibrium. The oxide products were analyzed chemically for cadmium content by standard polarographic methods. This showed the cadmium content of $CdFe_2O_4$ and $Cd_xZn_{1-x}Fe_2O_4$ mixed oxides to be within 0.5% of the expected stoichiometric values.

X-Ray Diffraction Analysis

Lattice parameters and diffraction intensities were obtained with an X-ray powder diffractometer equipped with a graphite-crystal monochromator (for the diffracted beam) and scintillation counter; Cu $K\alpha$ radiation was used throughout. Prolonged grinding of samples and back loading of the sample holder were performed in order to minimize (possible) preferred orientation effects (*14*).

The cubic lattice parameter, a_0, for each sample was determined from the corresponding diffractogram obtained at room temperature (293 ± 3 K) using NaCl (a_0 = 564.02 pm) as an internal standard. The cation distribution and oxygen parameter were

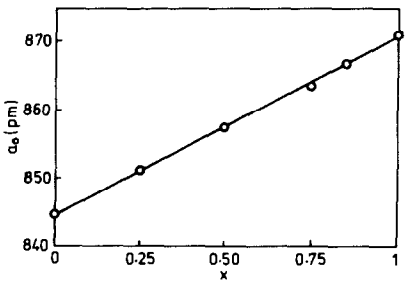

FIG. 1. Unit-cell length (a_0) as a function of composition (x) in $Cd_xZn_{1-x}Fe_2O_4$.

determined from the intensities of the (220), (311), (222), (400), (422), (333, 511), (440), (620), (533), (622), (642), (553, 731), (800), (555, 751), (662), (931), and (844) diffraction lines, which were scanned at a speed of 0.125° min^{-1} (2θ). Calculations were performed following the method proposed by Furuhashi *et al.* (*15*), which selects the best simulated structure by examining the degree of linearity of the relation (*16*).

$$\ln(I_{hkl}^{obs}/I_{hkl}^{calc}) = \ln K - 2B_{eff} \sin^2 \theta_{hkl}/\lambda^2. \quad (1)$$

Details of the experimental procedure, calculation method, and corresponding computer program were recently given elsewhere (*17*).

Results

Lattice Parameter and Oxygen Positional Parameter

The cubic unit-cell length, a_0, calculated from six high-angle diffraction lines ($2\theta > 50°$) for each sample, is plotted against the compositional parameter, x, in Fig. 1. The values of the oxygen positional parameter are presented in Fig. 2. Standard deviations (error bars) were calculated using a Monte Carlo method, described elsewhere (*17, 18*), which takes into account uncertainties due to stochastic fluctuations of the experimentally determined X-ray diffraction intensities.

Cation Distribution

Table I presents the cation distribution of each sample. Numbers in parentheses show the corresponding standard deviations, as determined by following the above-mentioned Monte Carlo method. Also shown in Table I is the thermal parameter, B_{eff}, and (in the last column) the square of the linear regression coefficient, r, for Eq. (1).

Interionic Distances

Knowledge of a_0 and u enables calculation of interionic distances. Cation–anion distances together with the distance of closest anion–anion approach are of major importance for a full discussion of cation distribution. Consideration of the geometry of the spinel-type structure leads to the following equations:

$$d_{AX} = a_0\sqrt{3}(u - \tfrac{1}{4}) \quad \text{tet bond} \quad (2)$$

$$d_{BX} = a_0(3u^2 - \tfrac{11}{4}u + \tfrac{43}{64})^{1/2} \quad \text{oct bond} \quad (3)$$

$$d_{XX} = a_0\sqrt{2}(2u - 1/2) \quad \text{tet edge} \quad (4)$$

$$d'_{XX} = a_0\sqrt{2}(1 - 2u) \quad \text{shared oct edge} \quad (5)$$

$$d''_{XX} = a_0(4u^2 - 3u + \tfrac{11}{16})^{1/2} \quad \text{unshared oct edge.} \quad (6)$$

Using the experimental values of a_0 and u shown in Figs. 1 and 2, Eqs. (2) to (6) lead to the values of interionic distances given in Table II. Also shown in this table are the radii, r_{tet} and r_{oct}, of the spheres which fit the tetrahedral and octahedral interstices.

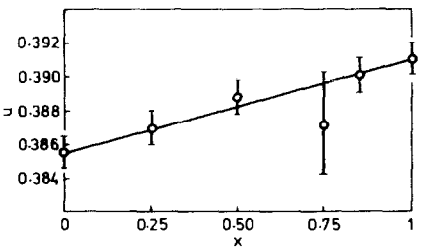

FIG. 2. Oxygen parameter (u) as a function of composition (x) in $Cd_xZn_{1-x}Fe_2O_4$.

TABLE I

CATION DISTRIBUTION IN $CdFe_2O_4$, $ZnFe_2O_4$ AND $Cd_xZn_{1-x}Fe_2O_4$ FERRITES

Mole fraction of Cd^{2+}, x	Cation distribution: Tetrahedral sites			Octahedral sites			Thermal parameter B_{eff}	r^2
	Cd^{2+}	Zn^{2+}	Fe^{3+}	Cd^{2+}	Zn^{2+}	Fe^{3+}		
0	—	0.79(1)	0.21(8)	—	0.21(1)	1.79(1)	0.53(1)	0.94
0.25	0.24(2)	0.55(9)	0.21(8)	0.01(2)	0.20(9)	1.79(8)	0.59(2)	0.90
0.50	0.50(1)	0.22(3)	0.28(3)	0.00(1)	0.28(3)	1.72(3)	0.49(1)	0.84
0.75	0.74(3)	0.04(6)	0.22(6)	0.01(3)	0.21(6)	1.78(6)	0.75(4)	0.84
0.85	0.78(1)	0.04(6)	0.18(4)	0.07(1)	0.11(6)	1.82(4)	0.53(2)	0.78
1	0.86(1)	—	0.14(1)	0.14(1)	—	1.86(1)	0.84(2)	0.94

These have been obtained from d_{AX} and d_{BX}, taking 138 pm as the radius of the O^{2-} ion (*19*).

Discussion

The X-ray diffraction pattern of each sample could be indexed completely on the basis of a single spinel-type cubic phase. No additional lines were found. Figure 1 shows that there is a continuous (approximately linear) variation of a_0 with the compositional parameter, x, in $Cd_xZn_{1-x}Fe_2O_4$. These results testify to the formation of a continuous series of solid solutions (at 1223 K) between $CdFe_2O_4$ and $ZnFe_2O_4$. The observed increase of a_0 as the cadmium content of the samples is raised is a direct consequence of the larger volume of the Cd^{2+} ion, compared with Zn^{2+}. According to Shannon (*19*) the ionic radii of Cd^{2+} and Zn^{2+} in fourfold (tet) and sixfold (oct) coordination are Cd^{2+}_{tet}, 78 pm; Cd^{2+}_{oct}, 95 pm; Zn^{2+}_{tet}, 60 pm; Zn^{2+}_{oct}; 74 pm. The a_0 value found for $CdFe_2O_4$ (a_0 = 871.0 pm) agrees, within experimental error, with a_0 = 869.96 pm given by the NBS (*20*). For $ZnFe_2O_4$ the present result (a_0 = 844.7 pm) is also consistent with the NBS (*21*) value: a_0 = 844.1 pm.

TABLE II

SELECTED INTERIONIC DISTANCES AND RADIUS OF THE TETRAHEDRAL AND OCTAHEDRAL INTERSTICES IN $Cd_xZn_{1-x}Fe_2O_4$

Mole fraction of Cd^{2+}, x	Tet edge (pm)	Oct edge: Shared (pm)	Oct edge: Unshared (pm)	r_{tet} (pm)	r_{oct} (pm)
0	324	272	299	60	65
0.25	330	272	302	64	65
0.50	337	269	304	68	65
0.75[a]	342	269	306	71	66
0.85	343	270	308	72	67
1	347	269	309	75	67

[a] For $Cd_{0.75}Zn_{0.25}Fe_2O_4$ calculations were done taking u = 0.3896, which corresponds to the linear plot in Fig. 2.

The experimental value of the oxygen parameter found for $CdFe_2O_4$ was u = 0.3910 (Fig. 2); no value for this parameter was found in the literature. For $ZnFe_2O_4$ we arrived at u = 0.3855 (Fig. 2) in good agreement with u = 0.385 ± 0.002 reported by Hastings and Corliss (*22*). Figure 2 shows that there is an approximately linear variation of u with the compositional parameter, x, along the series $Cd_xZn_{1-x}Fe_2O_4$. The deviation found at x = 0.75 is not considered to be significant, on account of its large standard deviation. The increasing value of u, as the cadmium content of the samples is raised, reflects the need for the structure to allow progressive expansion of the tetrahe-

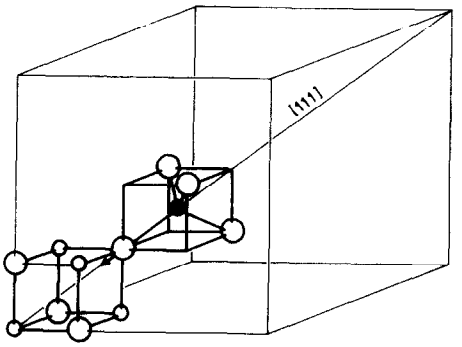

FIG. 3. Detail along a body diagonal of the spinel unit cell. The arrow indicates the direction in which the oxygen ion moves when $u > 0.375$. The black circle corresponds to a tetrahedrally coordinated cation. Small open circles denote octahedral cations and large open circles anions.

dral interstices in order to accommodate the more voluminous Cd^{2+} ions which replace Zn^{2+} precisely at these interstices, as shown in Table I. The detailed mechanism by which the tetrahedral interstices are enlarged when u increases above 0.375 is shown in Fig. 3. The anions move away from the nearest tetrahedral cation in a [111] direction, thus increasing the size of the tetrahedron relative to the ideal close-packed anion arrangement but without changing its $\bar{4}3m$ (T_d) symmetry. This expansion is reflected in the increasing length of both the tetrahedron edge and the mean radius (r_{tet}) of the tetrahedral interstices, as seen in Table II. It should be noted that only mean values can be obtained from the X-ray diffraction method used. This explains why in Table II r_{tet} is always smaller than 78 pm which would correspond to the radius of the tetracoordinated Cd^{2+} ion. Table I shows that, in addition to Cd^{2+}, the tetrahedral interstices also contain smaller Fe^{3+} ions (Fe^{3+}_{tet} = 49 pm) (*19*), and also Zn^{2+} ions up to $x = 0.75$.

No recent data were found regarding cation distribution in the single ferrites $CdFe_2O_4$ and $ZnFe_2O_4$. Investigations carried out long ago (*23–26*) suggest that both are normal spinels. The present results (Table I) show that at 1223 K (temperature from which the samples were quenched) $CdFe_2O_4$ and $ZnFe_2O_4$ are, respectively, 14 and 21% inverted.

The experimental results on cation distribution presented in Table I show that in the mixed ferrites $Cd_xZn_{1-x}Fe_2O_4$ coordination of the Fe^{3+} ion is very little affected by changes in chemical composition. Between the divalent ions, Cd^{2+} shows a stronger tetrahedral preference than Zn^{2+}. Thus, it is seen that up to $x = 0.75$ Zn^{2+} is replaced by Cd^{2+} exclusively at the tetrahedral interstices, the fraction of octahedrally coordinated Zn^{2+} ions remaining virtually unchanged. Cd^{2+} was also found to occupy tetrahedral sites in the mixed spinels $Cd_xCo_{1-x}Ga_2O_4$ (*27*), $Cd_xCu_{1-x}Al_2O_4$ (*28*), and $Cd_xCu_{1-x}Ga_2O_4$ (*12*). The d^{10} ions are expected to show tetrahedral preference in spinels because of the strong covalent contribution which can be developed between the anion and metal ions with closed shell electronic configuration (*6*). However, this argument applies equally well to Cd^{2+} and Zn^{2+}. The observed fact that Cd^{2+} only replaces Zn^{2+} at the tetrahedral interstices calls for a different explanation. We believe that steric effects are at operation.

The size of the tetrahedral interstices in the spinel structure is very sensitive to small displacements of the anions. Equation (2) shows that a small increase of the u parameter leads to a relatively large increase of the d_{AX} bond length and r_{tet}, as observed in Table II. However, r_{oct} is less sensitive to small changes of u. This is why the voluminous Cd^{2+} ion finds an easier accommodation at tetrahedral sites.

Now focusing our attention on the octahedral interstices, we must bear in mind that the displacement of the anions which enlarges u from its ideal value of 0.375 also causes a distortion of the octahedron from $m3m$ (O_h) to $\bar{3}m$ (D_{3d}) symmetry. For any

fixed value of a_0, this distortion tends to shorten the shared edge of the octahedra bringing the anions into close contact along those edges. Table II shows that in all the samples investigated the shared octahedral edge is about 270 pm long. This is not far from 276 pm which corresponds to twice the tetrahedral O^{2-} radius (*19*). Small differences are not considered to be significant, first because in the spinel structure (Fig. 3) polarization of the anion toward the tetrahedrally coordinated cation would facilitate closer anion approach along the shared octahedral edges. Second, and most important, because the tetrahedral sites are occupied by cations of different sizes (Table I) which produce local variations of the u parameter. X-ray diffraction (as used in the present work) only allows a mean value of u to be determined, thus precluding discussion in terms of very precise interionic distances. However, the fact remains that expansion of the tetrahedral interstices meets with the limitation imposed by concomitant shortening of the shared octahedral edge. This limitation could be overcome by increasing a_0 (Eq. (5)) but only at the expense of losing electrostatic energy. These considerations could provide the main argument to explain why in $CdFe_2O_4$, and $Cd_{0.85}Zn_{0.15}Fe_2O_4$, Cd^{2+} partially occupies octahedral sites (Table I) despite the strong tetrahedral preference shown by this ion.

References

1. D. R. Brown and E. Albers-Schoenberg, *Electronics* **26,** 146 (1953).
2. K. J. Standley, "Oxide Magnetic Materials," Oxford Univ. Press (Clarendon), London/New York (1972).
3. N. W. Grimes, *Phys. Technol.*, 22 (1975).
4. F. S. Galasso, "Structure and Properties of Inorganic Solids," Pergamon, Oxford (1970).
5. E. W. Gorter, *Philips Res. Rep. Eindhoven* **9,** 403 (1954).
6. G. Blasse, *Philips Res. Rep. Eindhoven,* Suppl. 3 (1964) and references therein.
7. J. S. Dunitz and L. E. Orgel, *J. Phys. Chem. Solids* **3,** 318 (1957).
8. A. Miller, *J. Appl. Phys.* **30,** 24S (1959).
9. C. Glidewell, *Inorg. Chim. Acta* **19,** L45 (1976).
10. P. Thompson and N. W. Grimes, *Philos. Mag.* **36,** 501 (1977).
11. P. Porta, F. S. Stone, and R. G. Turner, *J. Solid State Chem.* **11,** 135 (1974).
12. F. S. Stone, C. Otero Areán, J. S. Díez Viñuela, and E. Escalona Platero, *J. Chem. Soc. Faraday Trans. 1* **81,** 1255 (1985).
13. C. Otero Areán, J. S. Díez Viñuela, J. M. Rubio González, and A. Mata Arjona, *Mater. Chem.* **6,** 165 (1981).
14. H. P. Klug and L. E. Alexander, "X-Ray Diffraction Procedures," pp. 368, 369, Wiley, New York (1974).
15. H. Furuhashi, M. Inagaki, and S. Naka, *J. Inorg. Nucl. Chem.* **35,** 3009 (1973).
16. A. J. C. Wilson, *Nature (London)* **150,** 152 (1964).
17. J. M. Rubio González and C. Otero Areán, *J. Chem. Soc. Dalton Trans.*, 2155 (1985).
18. C. Otero Areán and J. M. Rubio González, *J. Solid State Chem.* **63,** 336 (1986).
19. R. D. Shannon, *Acta Crystallogr. Sect. A* **32,** 751 (1976).
20. ASTM Powder Diffraction File, Card No. 22-1063.
21. ASTM Powder Diffraction File, Card No. 22-1012.
22. J. M. Hastings and L. M. Corliss, *Rev. Mod. Phys.* **25,** 114 (1953).
23. E. J. W. Verwey and E. L. Heilmann, *J. Chem. Phys.* **15,** 174 (1947).
24. C. Guillaud, *J. Phys. Rad.* **12,** 239 (1951).
25. F. C. Romeijn, *Philips Res. Rep.* **8,** 304 (1953).
26. S. Hafner, *Schweiz. Mineral. Petrogr. Mitt.* **40,** 207 (1961).
27. C. Otero Areán and E. García Díaz, *Mater. Chem.* **7,** 675 (1982).
28. J. S. Díez Viñuela, C. Otero Areán, and F. S. Stone, *J. Chem. Soc. Faraday Trans. 1* **79,** 1191 (1983).